UC Santa Cruz
UC Santa Cruz Previously Published Works

Title

Pseudomonas aeruginosa PumA acts on an endogenous phenazine to promote self-resistance

Permalink

Journal

ISSN

Authors

Sporer, Abigail J
Beierschmitt, Christopher
Bendebury, Anastasia
et al.

Publication Date

DOI

Peer reviewed

MICROBIOLOGY
SOCIETY

Pseudomonas aeruginosa PumA acts on an endogenous phenazine to promote self-resistance

Abigail J. Sporer,[1]† Christopher Beierschmitt,[1]† Anastasia Bendebury,[1]† Katherine E. Zink,[2]† Alexa Price-Whelan,[1] Marisa C. Buzzeo,[3] Laura M. Sanchez[2] and Lars E. P. Dietrich[1],*

Abstract

The activities of critical metabolic and regulatory proteins can be altered by exposure to natural or synthetic redox-cycling compounds. Many bacteria, therefore, possess mechanisms to transport or transform these small molecules. The opportunistic pathogen *Pseudomonas aeruginosa* PA14 synthesizes phenazines, redox-active antibiotics that are toxic to other organisms but have beneficial effects for their producer. Phenazines activate the redox-sensing transcription factor SoxR and thereby induce the transcription of a small regulon, including the operon *mexGHI-opmD*, which encodes an efflux pump that transports phenazines, and *PA14_35160* (*pumA*), which encodes a putative monooxygenase. Here, we provide evidence that PumA contributes to phenazine resistance and normal biofilm development, particularly during exposure to or production of strongly oxidizing N-methylated phenazines. We show that phenazine resistance depends on the presence of residues that are conserved in the active sites of other putative and characterized monooxygenases found in the antibiotic producer *Streptomyces coelicolor*. We also show that during biofilm growth, PumA is required for the conversion of phenazine methosulfate to unique phenazine metabolites. Finally, we compare Δ*mexGHI-opmD* and Δ*pumA* strains in assays for colony biofilm morphogenesis and SoxR activation, and find that these deletions have opposing phenotypic effects. Our results suggest that, while MexGHI-OpmD-mediated efflux has the effect of making the cellular phenazine pool more reducing, PumA acts on cellular phenazines to make the pool more oxidizing. We present a model in which these two SoxR targets function simultaneously to control the biological activity of the *P. aeruginosa* phenazine pool.

INTRODUCTION

Microbes in mixed-species systems release small molecule antibiotics that support their fitness in multiple ways [1]. These compounds can inhibit the growth of other species, facilitate iron uptake, or act as electron acceptors for redox metabolism [2–5]. However, such functions require that the producing organisms tolerate the antibiotic and possess the machinery required to exploit the compound's beneficial effects. The transcription factor SoxR, which can be found in diverse bacterial phyla, regulates species-dependent sets of genes that are linked to antibiotic resistance and utilization, including those that encode efflux pumps and detoxifying enzymes [6–9]. Redox-active compounds can interact directly with the Fe–S cluster of the DNA-

bound SoxR dimer, leading to a conformational change in the promoter that induces the transcription of target genes [10, 11]. In bacteria that do not produce redox-active antibiotics, the SoxR regulon can confer protection from antibiotics produced by other species [7, 8, 12]. In bacteria that make these compounds, SoxR can mediate self-resistance [13].

In the opportunistic pathogen *Pseudomonas aeruginosa*, SoxR is activated by endogenous phenazines, redox-cycling compounds that are toxic to other organisms but have beneficial effects for their producer (Fig. 1a, b) [6, 14]. When other oxidants are not available, phenazines can accept electrons from *P. aeruginosa* metabolism and balance the intracellular redox state [5]. Reduced phenazines can shuttle

Fig. 1. Phenazine biosynthesis and self-resistance pathways. (a) The *P. aeruginosa* phenazine biosynthetic pathway. Redox potentials relative to the standard hydrogen electrode at pH 7.0 are given. PCA, phenazine-1-carboxylic acid; PCN, phenazine-1-carboxamide; 5-Me-PCA, 5-methylphenazine-1-carboxylic acid; PYO, pyocyanin. (b) Model of phenazine-mediated SoxR activation, with SoxR bound to the chromosomal locus between the genes *PA14_35160* (*pumA*) and *PA14_35170* (*soxR*). An additional SoxR target, the operon *mexGHI-opmD*, is shown below. (c) Phylogenetic distribution of orthologues of *phzM* (blue shading), *pumA* (yellow shading) and *mexG* (green shading) in the genus *Pseudomonas*.

outside of the cell and transfer electrons to oxidants that are available at a distance, including insoluble iron [15]. At physiological concentrations, the redox-balancing effects of phenazines are reflected macroscopically by colony biofilm morphology: phenazines promote the formation of a smooth colony, while phenazine deficiency (and therefore

electron acceptor limitation) promotes the development of wrinkle features, which increase the surface area-to-volume ratio of the colony and access to oxygen for resident cells [16, 17].

We study the *P. aeruginosa* PA14 SoxR regulon, which contains three chromosomal targets: the operon *mexGHI-opmD*, encoding an RND efflux pump; *PA14_35160*, encoding a putative monooxygenase; and *PA14_16310*, encoding a putative MFS transporter [6, 14]. *PA14_35160* is orthologous to the gene *PA2274* in *P. aeruginosa* strain PAO1 and is chromosomally adjacent to the gene encoding SoxR. In a prior study, we found that Δ*soxR*, Δ*mexGHI-opmD* and Δ*PA14_35160* mutants are more sensitive to phenazine methosulfate (PMS), a structural analogue of the reactive *P. aeruginosa* product 5-methylphenazine-1-carboxylic acid (5-Me-PCA), than the wild-type. Results from our follow-up experiments implicated the MexGHI-OpmD pump in 5-Me-PCA efflux [13]. However, this work also suggested that the *PA14_35160* gene product contributed to *P. aeruginosa* phenazine resistance. Here, we show that PA14_35160 transforms endogenous phenazines, leading to physiological effects that support normal community development, and suggest the name PumA (phenazine utilizing monooxygenase A) for this protein. These results further our understanding of *P. aeruginosa* phenazine metabolism in the context of biofilm growth.

METHODS

Strains and culture conditions

The strains used in this study are listed in Table S1 (available in the online version of this article). For preculturing and genetic manipulation, bacteria were grown at $37\,^{\circ}$C in lysogeny broth (LB) with shaking at 250 r.p.m. (Forma Orbital Shaker, Thermo Scientific) or on LB solidified with agar ($15\,\text{g\,L}^{-1}$) [18]. For selection during genetic manipulation, gentamicin was added to the medium at $15\,\mu\text{g\,mL}^{-1}$ for *Escherichia coli* or $100\,\mu\text{g\,mL}^{-1}$ for *P. aeruginosa*. Carbenicillin was added to the medium at $300\,\mu\text{g\,mL}^{-1}$ for *P. aeruginosa*.

To characterize phenazine sensitivity and biofilm development, colonies were grown at $30\,^{\circ}$C on 1 % tryptone and 1 % agar, containing $40\,\mu\text{g\,mL}^{-1}$ Congo red and $20\,\mu\text{g\,mL}^{-1}$ Coomassie blue where indicated.

Strain construction

The strains used in this study are listed in Table S1, while the plasmids used in this study are listed in Table S2 and the primers used for the construction of plasmids are listed in Table S3. The plasmids for deletion and gene replacement were generated using the yeast gap repair method as described previously [19, 20]. Markerless deletions of *pumA* were generated as described previously by homologous recombination in various PA14 strain backgrounds [20]. The same approach was used to complement Δ*pumA* using complementation plasmids. The final clones were verified by PCR and sequencing.

GFP reporter strains were constructed using plasmid pLD2726, generated by inserting the 448 bp of the *mexG* promoter between an engineered SpeI and XhoI site into a pSEK103 plasmid backbone using the primers indicated in Table S3. Strains expressing GFP under the control of the *mexG* promoter were generated by homologous recombination of plasmid pLD2762 into the neutral attB site on the PA14 chromosome. Plasmids were transformed into *E. coli* strain UQ950, verified by sequencing and moved into PA14 using biparental conjugation with *E. coli* strain S17-1. PA14 single recombinants were selected on M9 minimal medium agar plates ($47.8\,\text{mM}$ Na$_2$HPO$_4\bullet$7H$_2$O, $22\,\text{mM}$ KH$_2$PO$_4$, $8.6\,\text{mM}$ NaCl, $18.6\,\text{mM}$ NH$_4$Cl, $1\,\text{mM}$ MgSO$_4$, $0.1\,\text{mM}$ CaCl$_2$, $20\,\text{mM}$ sodium citrate dihydrate, 1.5 % agar) containing $100\,\mu\text{g\,mL}^{-1}$ gentamicin. The plasmid backbone was resolved out of PA14 using Flp/FRT recombination by the introduction of the pFLP2 plasmid [21] and selected on M9 minimal medium agar plates containing $300\,\mu\text{g\,mL}^{-1}$ carbenicillin and further on LB agar plates without NaCl and modified to contain 10 % sucrose. The presence of *gfp* in the final clones was confirmed by PCR.

Colony morphology assay

Ten microlitres of overnight precultures were spotted on 1 % tryptone + 1 % agar containing $40\,\mu\text{g\,mL}^{-1}$ Congo red and $20\,\mu\text{g\,mL}^{-1}$ Coomassie blue ($60\,\text{mL}$ in a 9 cm square plate) and incubated at $25\,^{\circ}$C, >95 % humidity. The colonies were imaged daily using an Epson 11000XL scanner. For the onset of wrinkling determination, overnight precultures were diluted 1 : 100 and grown to the mid-log phase before $10\,\mu\text{L}$ of the culture was spotted onto the agar plates. Time-lapse movies of colony development were assembled from images taken using a Logitec c930e web-camera triggered at 15 min intervals by a custom Labview program.

PMS sensitivity

Cultures were grown in LB for 16 h at $37\,^{\circ}$C with continuous shaking at 250 r.p.m. After 16 h, $10\,\mu\text{L}$ of culture was spotted on morphology agar supplemented with $600\,\mu\text{M}$ PMS and dried. The plates were incubated in the dark at $25\,^{\circ}$C. The colonies were imaged at indicated time points using an Epson 11000XL scanner. For the quantification of colony-forming units (c.f.u.s), $10\,\mu\text{L}$ of overnight LB precultures was spotted on filter disks overlaid on the same morphology agar +/−$600\,\mu\text{M}$ PMS. After 48 h of growth, filter disks with the colonies were lifted from the agar using sterile forceps and added to a 1.5 mL screw-cap tube containing 1 mL phosphate-buffered saline (PBS) and disrupted with 3 mm zirconium beads in a BeadRupter 12 homogenizer (Omni International, Inc.) for 90 s on the 'high' setting. Dilutions of homogenized biofilms in PBS were plated on 1 % tryptone, 1 % agar plates and incubated overnight at $37\,^{\circ}$C, and the colony-forming units were then counted.

Statistical analysis

Data analysis was performed using GraphPad Prism version 7 (GraphPad Software, La Jolla, CA, USA). Values are expressed as mean ± SD. The statistical significance of the

data presented was assessed with the two-tailed unpaired Student's *t*-test. Values of $P \leq 0.05$ were considered significant (*$P \leq 0.05$; **$P \leq 0.005$; ***$P \leq 0.0005$).

Protein structure prediction and presentation

The structures for EcaB and PumA were predicted using the Phyre2 homology modelling engine [22]. These structures and ActVA-Orf6 (PDB: 1LQ9; [23]) were visualized with the PyMOL molecular graphics system, version 2.0, Schrödinger, LLC [24].

Imaging mass spectrometry

The indicated *P. aeruginosa* strains were streaked from frozen stocks onto plates containing 1 % tryptone (Bacto) and 1 % agar. After 24 h of incubation at 30 °C, colonies were used to inoculate 5 mL LB cultures, which were shaken at 225 r.p.m. at 30 °C for 24 h. Five microlitres of each liquid culture was plated onto separate thin plates supplemented with 200 µM PMS. PA14 Δ*phz* was grown on both supplemented and unsupplemented agar plates. The plates were incubated for 5 days in a sealed container at room temperature in the absence of light.

After 5 days of incubation, the colonies were physically excised on mats of the agar using razor blades and scalpels and laid flat on a steel MALDI plate (Bruker 96-spot ground). Two agar controls were also placed on the plate: one LB agar alone and one supplemented with 200 µM PMS. A MALDI matrix [50:50 α-cyano-4-hydroxycinnamic acid (CHCA): 2,5- dihydroxybenzoic acid (DHB)] was applied using a a 53 µm stainless steel sieve (Hogentogler and Co., Inc.) onto the colonies and agar. The steel plate was placed uncovered in a 37 °C oven for 12 h or until dried. Excess matrix was removed using air. Then 1 µL of phosphorus red (1 mg mL^{-1}) was spotted on an agar-free area of the steel plate as a calibration standard. The data were gathered in reflectron positive mode, from 100 to 2000 Da. The raster width across the sample was 200 µm. FlexImaging 4.1 was used with flexControl 3.4 to set up the IMS analysis, and regions of interest (ROI) were manually designated for each culture or growth condition. The laser power and detector gain were set to 30 % and 3.0×, respectively. Five hundred shots were taken at 2000 Hz at each raster spot, with the laser width (smartbeam parameter set) set to 2 (small). The resulting spectra were analysed using FlexImaging 4.1 after normalization to root mean square (RMS).

Compound isolation and structure elucidation

Relevant *P. aeruginosa* strains were streaked from frozen stocks onto plates containing 1 % tryptone, 1 % agar and incubated overnight at 30 °C. After 24 h, individual colonies were transferred into culture tubes containing 5 mL of liquid LB (10 g tryptone, 5 g yeast extract, 10 g NaCl in 1 L MilliQ water, pH 7.5) and shaken at 225 r.p.m. and 30 °C. After 24 h, the liquid culture was diluted to an OD (500 nm) of 0.05 into 30 mL of LB. After 24 h, the liquid culture was again used to inoculate 1 L of LB to an OD (500 nm) of 0.05. At an OD (500 nm) of 0.4–0.5 (early stationary phase), 200 µM of phenazine methosulfate (PMS) in MilliQ H_2O

was added to the culture. Alongside the 1 L bacterial culture was an uninoculated 1 L flask of LB, also with PMS added. The culture flasks were capped with milk filters and autoclave paper, secured with a rubber band and incubated for 48 h. The soluble compounds from the 1-L culture were then extracted using Amberlite-XAD 16 resin (20 g L^{-1} of medium). The resin was shaken in the culture flask for 1 h at 225 r.p.m. and the resin and cells were collected by vacuum filtration. The resin, cells and filter paper were then back-extracted using 100–200 mL of MeOH. The organic material was dried *in vacuo* and separated based on polarity under solid-phase extraction (SPE) using a Supelco Discovery DSC-18 cartridge (20 mL, 5 g). The material was subjected to seven elution steps, six covering a gradient of MeOH/H_2O (A: 10 % MeOH, B: 20 % MeOH, C: 40 % MeOH, D: 60 % MeOH, E: 80 % MeOH, F: 100 % MeOH) and the seventh 100 % EtOAc. All fractions were dried *in vacuo*.

Fractions C, D and E contained pumazine when checked by dried droplet (DD) on the matrix-assisted laser desorption/ ionization time-of-flight (MALDI-TOF)mass spectrometer. Fraction E was subjected to liquid chromatography (LC)/ tandem mass spectrometry (MS/MS) (LC-MS/MS) at a gradient of 40–100 % MeOH/H_2O over 30 min. Pumazine was detected at 20.5 min (approximately 85 % MeOH). Fraction E was subjected to an initial isocratic isolation at 72 % MeOH (0.2 % FA) using RP-HPLC on a C18 column (Phenomenex Kinetex; 5 µm C18, 100 Å, 150×4.6 mm). Eluents between 3 and 4 min were collected, dried *in vacuo* and further separated by HPLC using isocratic conditions, 50 % MeOH (0.2 % FA) over 12 min, on a biphenyl column (Phenomenex Kinetex; 5 µm biphenyl, 100 Å, 150×4.6 mm). Under these conditions, pumazine eluted at 8.1 min and the resulting red fraction was dried *in vacuo* and protected from light and air. The collected compound was a bright magenta colour when dried.

Pumazine

Pink solid; [α]^{20} 0 (*c* 0.1, MeOH); UV (MeOH) λ$_{max}$ (log ε) 280 (10.88) nm, 380 (11.02) nm and 508 (11.14) nm; IR (glass, cm^{-1}) 3413, 2980, 1596 and 1384; ^{1}H NMR (400 MHz, DMSO-d$_6$) δ 7.26 (d, 1 h, *J*=8.5 Hz), 7.98 (d, 1 h, *J*=8.5 Hz); High resolution electrospray ionization mass spectrometry (HRESIMS) *m/z* [M+H]$^+$ 275.0308 (calc. $C_{12}H_7N_2O_6$, 275.0304).

Nuclear magnetic resonance (NMR) spectra were collected on a Bruker AVII 400 MHz spectrometer equipped with a 5 mm Z-gradient BBO probe with an internal standard of tetramethylsilane (TMS) and referenced to residual solvent proton signals (ΔH 2.50 for DMSO). HPLC purifications were performed with an Agilent Technologies 1260 Infinity HPLC. All solvents were Optima grade and were used without further purification. Direct infusion was performed on a LCQ Advantage Max (Thermo Finnigan). LC-MS/MS experiments were performed on an 6300 ion trap (Agilent Technologies). HRESIMS data were collected on both an 6550 i-Funnel Q-TOF (Agilent Technologies) and an

Impact II Q-TOF (Bruker Daltonics, Billerica, MA). UV-visible data were collected on a UV-2401PC UV/vis spectrophotometer (Shimadzu). IR data were collected on a Thermo Scientific Nicolet 6700 FT-IR. Optical rotation data were collected on a 241 Polarimeter (Perkin Elmer). NMR modelling was performed using NMR Predict (nmrdb.org).

Cyclic voltammetry

Electrochemical measurements were performed on a μAutolab Type III potentiostat (Eco Chemie, Metrohm USA, Riverview, FL, USA) in a Faraday cage. The electrochemical cell contained a glassy carbon (d=2.4 mm) disk working electrode, a platinum wire counter electrode and a Ag/AgCl reference electrode (BASi, West Lafayette, IN, USA). The electrodes were mechanically polished with 1.0 and 0.3 μm alumina slurries (Buehler, Lake Bluff, IL, USA), after which they were rinsed with distilled water. Solutions were purged with ultra-high purity N_2 (g) prior to and during the experiment. Cyclic voltammograms were recorded at a scan rate of $0.1\ Vs^{-1}$ for five consecutive cycles. Potentials are reported versus Ag/AgCl. Phenazine methosulfate was obtained from TCI America and pumazine was purified as indicated in the mass spectrometry methods text above. Both compounds were tested at a concentration of 15 μM. The aprotic solvent system used consisted of dimethyl sulfoxide (DMSO) with 100 mM tetrabutylammonium hexafluorophosphate (TBAPF$_6$); the protic solvent system consisted of 20 mM MOPS (pH 7.2) with 100 mM potassium chloride. All chemicals were purchased from Sigma Aldrich at analytical (>99.5 %) purity and used without further purification.

RESULTS AND DISCUSSION

Genes for N-methylated phenazine production and those implicated in resistance co-occur in pseudomonad species

We previously observed that SoxR-mediated regulation is important for normal *P. aeruginosa* PA14 biofilm development and growth under conditions where N-methylated phenazines are produced or added to the growth medium [13]. We therefore hypothesized that the ability to produce N-methylated phenazines and proteins that protect from these compounds would correlate in *Pseudomonas* species. In *P. aeruginosa*, phenazine methylation is catalyzed by the enzyme PhzM, which converts phenazine-1-carboxylic acid (PCA) to 5-Me-PCA [25] (Fig. 1a). We used the *Pseudomonas* Genome Database [26] to search for orthologues of SoxR and PhzM, and proteins that are expressed in response to SoxR activation. We found 94 species with SoxR orthologues (Fig. 1c). Orthologues of PhzM were present in only four species, all of which also contained SoxR. We found a perfect overlap between genomes that contained orthologues of *phzM* and *PA14_35160* (*pumA*), which encodes a putative monooxygenase and is regulated by SoxR. Orthologues of *mexG*, which is also regulated by SoxR and encodes a component of the efflux pump that protects *P. aeruginosa* from N-methylated phenazines [13], were found in these same four

genomes and an additional five genomes, all of which also contained *soxR*. Thus, the potential to produce methylated phenazines is a relatively rare feature among pseudomonad species, and it tends to co-occur with genes that provide protection from these products.

A mutant lacking PA14_35160 (PumA) shows altered growth and biofilm development in response to synthetic and endogenous N-methylated phenazines

The *P. aeruginosa* phenazine biosynthetic pathway is branched and yields at least four different phenazine products during biofilm growth on our standard medium (1 % tryptone, 1 % agar) (Fig. 1a) [27, 28]. We found that 5-Me-PCA has more pronounced effects on SoxR-mediated gene expression and colony morphogenesis than other *P. aeruginosa* phenazines [13]. Because 5-Me-PCA is unstable, we use the synthetic analogue PMS to characterize the effects of specific gene deletions on *P. aeruginosa*'s responses to methylated phenazines. We conducted a time course examining the colony development of wild-type PA14 and mutants representing SoxR and SoxR-regulated genes. As previously reported, we observed that $\Delta pumA$ colony biofilms show defective growth on medium containing 600 μM PMS and that *pumA* and *mexGHI-opmD* together account for the full degree of protection from PMS afforded by the SoxR regulon (Fig. 2a) [13].

Although N-methylated phenazines such as PMS are toxic at high concentrations, our previous work indicated that they can provide a physiological benefit at lower concentrations by acting as alternative electron acceptors for cells in oxygen-limited regions of biofilms [13]. This cellular redox balancing promotes the formation of smooth colonies, while electron acceptor limitation promotes colony wrinkling [29]. To determine whether PumA is involved in the morphological response to an endogenous N-methylated phenazine, we generated a series of combinatorial mutants with deletions in *phz* genes and SoxR target genes. The mutants shown in Fig. 2(b) overproduce 5-Me-PCA due to a deletion in *phzH* (Fig. 1a). We observed that the deletion of *pumA* in this background stimulated colony wrinkling, while the deletion of *mexGHI-opmD* had the opposite effect (Fig. 2b). To assess whether the earlier onset of wrinkling in $\Delta pumA$ strains could be attributed specifically to the effect of methylated phenazines, we compared the colony phenotypes of $\Delta pumA$ in the presence and absence of the methyltransferase gene *phzM*. Consistent with the notion that PumA acts on methylated phenazines, we did not find a significant effect on colony development in a *phzM* deletion background (Figs S1a and 2c). Accordingly, we also found that deletion of *pumA* in the Δphz background did not affect colony morphology in the absence of phenazines, but led to enhanced colony wrinkling when the strains were grown on the synthetic methylated phenazine PMS at all concentrations of PMS tested (Fig. S1b). Taken together, these results implicate PumA in *P. aeruginosa* phenazine resistance and phenazine-mediated repression of colony wrinkling. Our
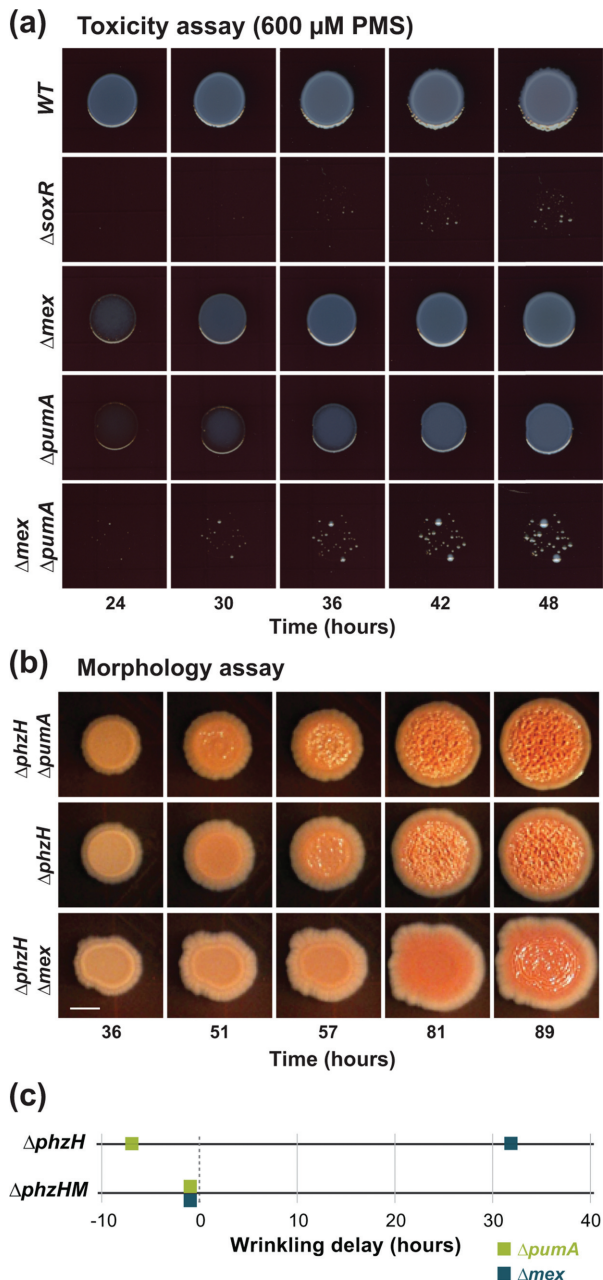
(a) Toxicity assay (600 µM PMS)

(b) Morphology assay

(c)

Fig. 2. PumA contributes to *P. aeruginosa* phenazine resistance and colony development. (a) Growth of WT PA14 and mutants on medium containing 600 µM PMS. (b) Colony biofilm development of Δ*pumA* and Δ*mexGHI-OpmD* in a strain background that overproduces methylated phenazines (Δ*phzH*). Deletion of *pumA* stimulates colony wrinkling, while deletion of *mexGHI-opmD* inhibits it, under this condition. The images were taken from time-lapse movie S1. (c) Onset of wrinkling relative to parent strains Δ*phzH* (top) and Δ*phzHM* (bottom) for the indicated mutants. Deletion of *pumA* stimulates colony wrinkling, while deletion of *mexGHI-opmD* ('*mex*') inhibits colony wrinkling. This wrinkling differential is specific to the overproduction of N-methylated phenazines, as the onset of wrinkling in the Δ*phzH*Δ*phzM* background is not significantly different from that of the parent for Δ*pumA* or Δ*mex*. The onset of wrinkling was determined from time-lapse movies S1 and S2.

work suggests that *mexGHI-opmD* deletion leads to increased retention of 5-Me-PCA and other N-methylated phenazines, thereby leading to a more oxidized cellular redox state and inhibition of colony wrinkling. The fact that a *pumA* deletion stimulates colony wrinkling suggests that this mutant harbours a more reduced cellular redox state. We hypothesize that PumA converts 5-Me-PCA and/or other N-methylated phenazines to products with potentials that are more oxidizing.

PumA is a putative monooxygenase

PumA is orthologous to two separate proteins found in *Streptomyces coelicolor*: ActVA6-Orf6 and EcaB. ActVA6-Orf6 has been crystallized as a dimer and acts as a monooxygenase in the synthesis of a polyketide called actinorhodin [23, 30]. This redox-active antibiotic affects *S. coelicolor* colony morphogenesis in a similar manner to phenazines in *P. aeruginosa* [6]. Actinorhodin also activates *S. coelicolor* SoxR, which controls the expression of a six-gene regulon that includes *ecaB* [9]. The conserved regulation of PumA and EcaB expression by SoxR suggests that these two putative monooxygenases may have similar functions. EcaB is approximately twice the length of PumA (234 vs 125 amino acid residues). This increased size is likely due to an internal duplication, as the EcaB monomer consists of two domains that are each homologous to PumA (Fig. 3a). We will refer to the N-terminal and C-terminal domains of EcaB as 'EcaB$_N$' and 'EcaB$_C$', respectively. In a previous study, Sciara *et al.* identified four active site residues, which we have highlighted in the ActVA-Orf6 shown in Fig. 3(a) [23]. Two of these, an asparagine and a tryptophan, are well conserved between orthologues and were proposed to be required for catalysis, while the two poorly conserved tyrosine residues were proposed to confer substrate specificity in divergent monooxygenases [23]. Although EcaB$_N$ contains a histidine in place of the catalytic asparagine residue, both PumA and EcaB$_C$ contain putative active sites (Fig. 3b). Given the similarities between PumA and the C-terminal domain of EcaB, we were interested in examining whether EcaB and EcaB$_C$ could functionally replace PumA *in vivo*.

We tested whether EcaB, EcaB$_C$, or a version of PumA with a mutant active site (i.e. lacking the conserved asparagine and tryptophan residues) could confer PMS tolerance in a Δ*phz*Δ*pumA* background by growing strains as biofilms on medium with or without 600 µM PMS for 4 days, harvesting and homogenizing the biofilms, and plating for colony-forming units. In this assay, Δ*phz*Δ*pumA* showed a 1.5 log decrease in c.f.u.s for biofilms grown on 600 µM PMS compared to those grown on tryptone alone (Fig. 3c). Resistance to PMS was rescued by complementation with intact PumA (Δ*pumA* :: *pumA*). When Δ*phz*Δ*pumA* was complemented with a catalytic site mutant of PumA, PumA^{N76A,W80A}, there was no observable rescue of PMS resistance. Complementation of Δ*phz*Δ*pumA* with both full-length *ecaB* and *ecaB$_C$* resulted in partial rescue on 600 µM PMS. These results suggest that EcaB and PumA could play similar roles in antibiotic self-resistance in their respective organisms.
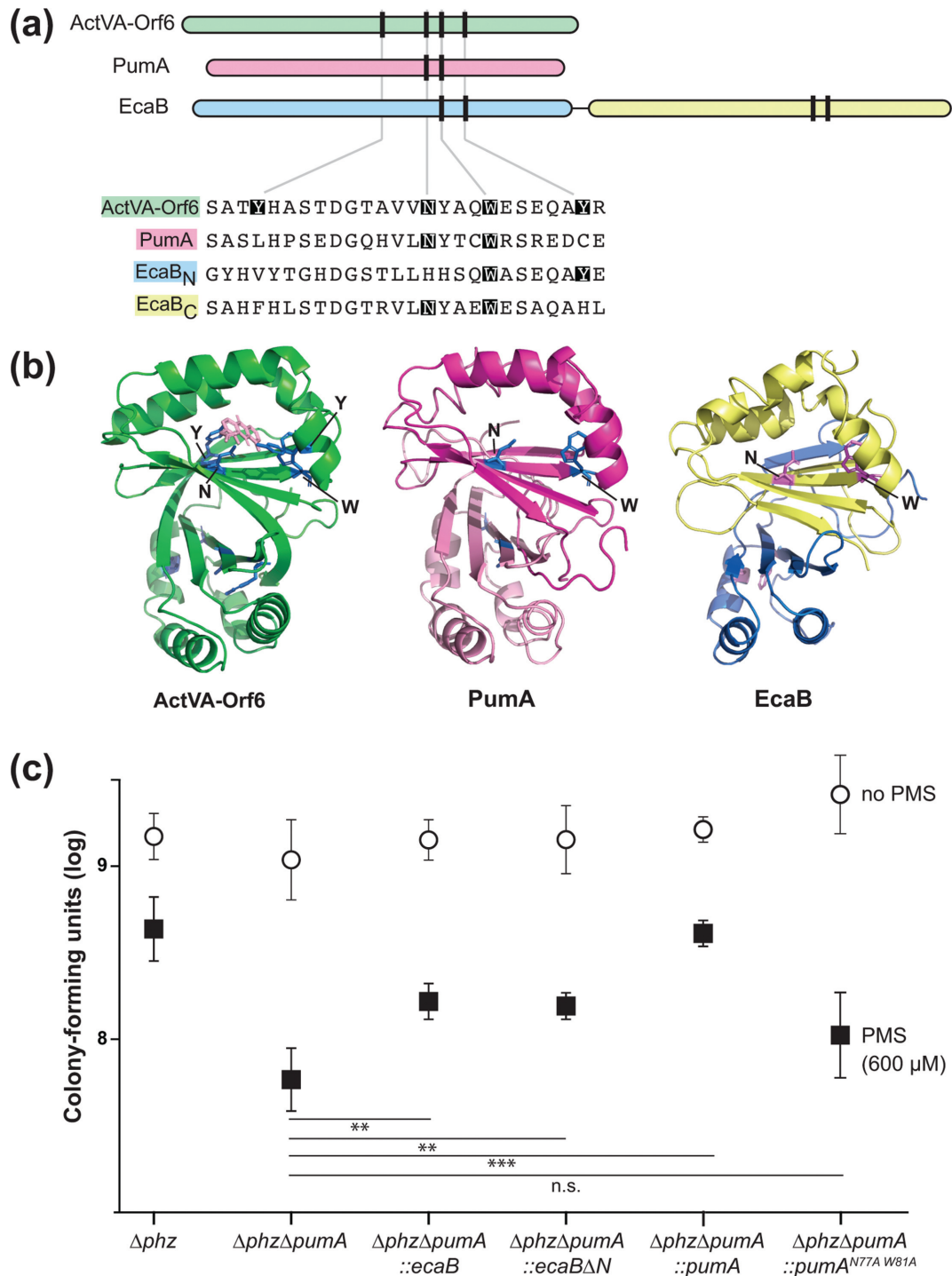
Fig. 3. PumA shows homology to the *S. coelicolor* monooxygenase ActVA-Orf6 and the *S. coelicolor* protein EcaB, which also confers PMS tolerance in *P. aeruginosa*. (a) Top: domain architectures of the *S. coelicolor* monooxygenase ActVa-Orf6, *P. aeruginosa* PumA and the *S. coelicolor* SoxR-target EcaB. Vertical lines represent the locations of residues that are important for ActVA-Orf6 activity. Bottom: alignment of selected regions from *S. coelicolor* ActVA-Orf6, *P. aeruginosa* PumA and *S. coelicolor* EcaB. Catalytic site residues identified in *S. coelicolor* ActVA-Orf6 that are conserved are indicated with shading. (b) Structure of *S. coelicolor* ActVA-Orf6 (left), and threaded structures of *P. aeruginosa* PumA (middle) and *S. coelicolor* EcaB (right). The domains are colour-coded as in panel (a). (c) Assay for tolerance to 600 μM PMS. Biofilms were grown on 1 % tryptone+1 % agar for 4 days, and then whole colonies were homogenized for colony-forming unit plating. The error bars represent the standard deviation of biological quadruplicates. *P*-values were calculated using unpaired, two-tailed *t*-tests (*P*>0.05 was considered not significant; **$P \leq 0.005$; ***$P \leq 0.0005$).
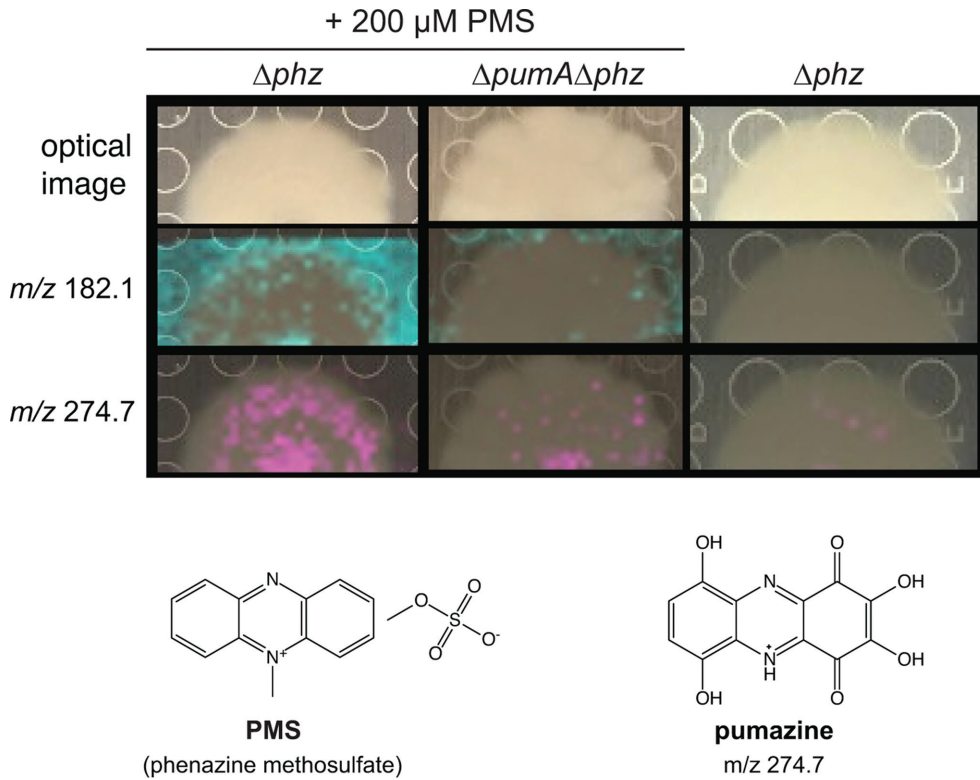
Fig. 4. Identification of PumA-dependent metabolites. Top: optical images of colony biofilms and imaging mass spectrometry results showing distribution of metabolites with the indicated mass-to-charge (*m/z*) ratios (in cyan or fuschia) overlaid on colony images. Colonies were grown for 5 days on 1 % tryptone and 1 % agar. PMS was added to the medium where indicated. Bottom: structure for PMS and predicted structure for pumazine.
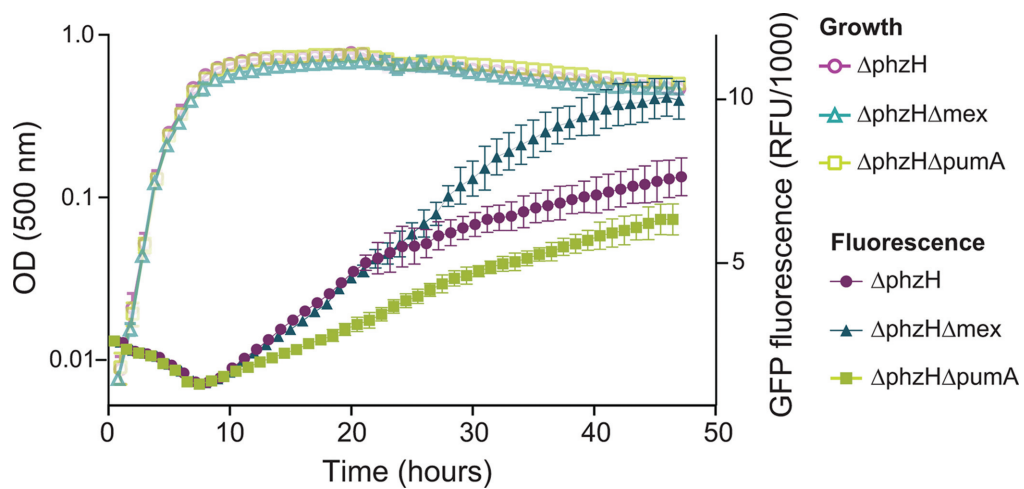

Fig. 5. PumA and MexGHI-OpmD divergently affect SoxR activation. In a mutant background that overproduces N-methylated phenazines (5-Me-PCA and derivatives), Δ*mex* strains show increased expression of a SoxR-regulated GFP reporter, while Δ*pumA* strains show decreased expression. Because SoxR is activated by oxidized phenazines, these results indicate that the phenazine pool is more oxidizing in Δ*mex* strains and more reducing in Δ*pumA* strains.

PumA modifies PMS during growth in biofilms and liquid cultures

In *S. coelicolor*, ActVA-Orf6 catalyzes the oxidation of an intermediate in actinorhodin biosynthesis. This reaction converts 6-deoxydihydrokalafungin into dihydrokalfungin (quinone) [23]. By analogy, we hypothesized that PumA could transform phenazines. We used imaging mass spectrometry (IMS) to identify PumA-dependent metabolites produced by biofilms grown on medium containing 200 µM PMS (Figs 4 and S2) [31]. We found two metabolites, *m/z* 182.1 and *m/z* 274.7, that (a) showed increased abundance in Δ*phz* biofilms grown on PMS when compared to Δ*phz*Δ*pumA* biofilms grown on PMS, and (b) were absent from Δ*phz* biofilms grown on PMS-free medium. To purify enough compound to enable characterization, we grew Δ*phz* and Δ*phz*Δ*pumA* as shaken liquid cultures in medium containing 200 µM PMS and analysed the culture supernatants for PumA-specific metabolites. We found that the *m/z* 274.7 compound identified by IMS of biofilms was also produced during growth in liquid culture. Species *m/z* 182.1 was not observed in liquid culture and was therefore not pursued for further structure elucidation studies.

We purified the *m/z* 274.7 compound from culture supernatants and determined its structure using LC-MS/MS fragmentation and NMR (Fig. S3a). This metabolite, henceforth called pumazine, is a highly modified phenazine core with six additional oxygen atoms substituted at six different aromatic carbons. Deuterium exchange indicates that four of the oxygen substituents are hydroxyl groups (Fig. S3b) and the remaining two oxygens are in keto form (quinone). We further characterized the purified pumazine compound by UV-visible spectrophotometry and cyclic voltammetry. The absorbance spectra of natural phenazines often show features in the ranges of 250–290 and 350–400 nm, with a subset showing a peak between 400–600 nm, consistent with colouration [32, 33]. Pumazine displays characteristic phenazine absorbance peaks at 280, 375 and 515 nm (Fig. S4a). We examined the redox activity of pumazine by cyclic voltammetry in aprotic (0.1 M TBAPF$_6$/DMSO) and protic (20 mM MOPS buffer, pH 7.2) solvent systems. A quasi-reversible redox couple is observed on glassy carbon electrodes that is shifted reductively relative to PMS (ΔE$_{mid}$ ~360 mV in DMSO; ΔE$_{mid}$~220 mV in MOPS buffer) and, by inference, to 5-Me-PCA (Fig. S4b, c). We attribute the substantial potential shift to the extent of substitution on the phenazine core [34–36].

PumA acts on endogenous phenazines

Studies in our laboratory indicated that *P. aeruginosa* colony morphogenesis is linked to the cellular redox state [16, 37] and that phenazine-dependent repression of colony wrinkling is mediated in part by the oxidizing effects of these compounds [38]. We therefore hypothesized that the early onset of wrinkling in Δ*pumA* mutants was stimulated by a shift in the stoichiometry of the intracellular phenazine pool. We use a fluorescent reporter of *mexGHI-opmD* expression, P$_{mexG}$-GFP, as a proxy for SoxR activity. We

observed that Δ*phzH* mutants, which produce increased amounts of 5-Me-PCA, show the highest levels of SoxR activation when compared to strains with intact or otherwise altered phenazine biosynthetic pathways [13, 39]. We have also seen that removal of the MexGHI-OpmD efflux pump, which transports 5-Me-PCA, further induces *mexGHI-opmD* expression. As SoxR is activated by oxidation of its Fe–S cluster, these results are consistent with the fact that 5-Me-PCA has the most oxidizing potential of all of the well-characterized *P. aeruginosa* phenazines [36]. To test whether the endogenous phenazine pool is affected by the Δ*pumA* mutation, we moved the P$_{mexG}$-GFP reporter into a Δ*phzH*Δ*pumA* mutant and measured fluorescence during growth in well-mixed liquid cultures. This strain showed lower levels of GFP expression, suggesting that it has a phenazine pool with a more reducing potential than its parent strain (Fig. 5).
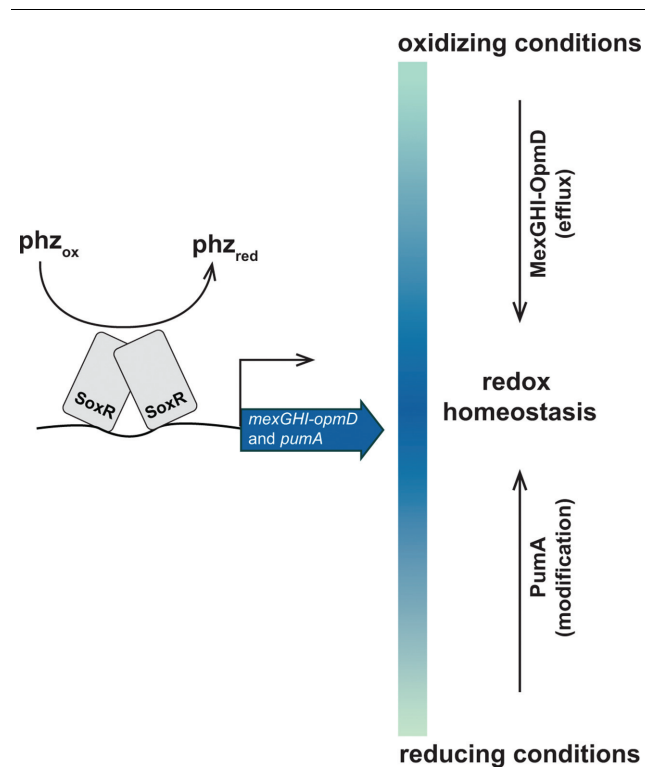

Fig. 6. Model depicting the roles of SoxR-regulated proteins in modulating the cellular phenazine pool. Phenazine-mediated oxidation of SoxR activates the transcription of target loci, including the *mexGHI-opmD* operon (encoding an efflux pump), and *PA14_35160* (*pumA*) (encoding a putative monooxygenase). Mutant colony morphotypes and reporter gene expression data indicate that these SoxR targets have differential effects on the redox potential of the cellular phenazine pool: while MexGHI-OpmD-mediated efflux leads to phenotypes consistent with a more reducing phenazine pool, PumA activity leads to phenotypes consistent with a more oxidizing one. We propose that these proteins work simultaneously to ensure optimal phenazine self-resistance in *P. aeruginosa* PA14.

The measured midpoint potential of pumazine is much more negative than the values reported for N-methylated phenazines (Fig. S4b, c) [34–36]. If pumazine were the primary product of PumA, we would therefore expect the Δ*pumA* mutation to lead to a more oxidized environment. However, *pumA* deletion leads to earlier wrinkling (Fig. 2b, c) and decreased SoxR reporter activity (Fig. 5), effects that are consistent with a more reduced cellular redox state. These findings indicate that pumazine is not the direct product of PumA activity, which is plausible given the known reactivity of modified phenazines. Nevertheless, our results suggest that PumA acts on endogenous phenazines to modulate cellular redox conditions and prompt us to propose a model in which the SoxR regulon supports redox homeostasis by modulating the phenazine pool: while the efflux pump MexGHI-OpmD counteracts excessively oxidizing conditions by exporting methylated phenazines, PumA modifies endogenous *P. aeruginosa* phenazine structures and/or levels in a way that shifts the conditions inside the cell to a more oxidizing state (Fig. 6).

Concluding remarks

Our results suggest that PumA acts on endogenous and exogenous N-methylated phenazines to yield a phenazine pool that supports *P. aeruginosa* growth and colony development. They also indicate that EcaB could act similarly on antibiotics produced or taken up by *S. coelicolor*. The SoxR-mediated induction of modifying enzymes may therefore represent a conserved mechanism of self-resistance in divergent bacterial phyla.

Conflicts of interest
The authors declare that there are no conflicts of interest.

References
1. **Bernier SP, Surette MG.** Concentration-dependent activity of antibiotics in natural environments. *Front Microbiol* 2013;4:20.
2. **Davies J.** Specialized microbial metabolites: functions and origins. *J Antibiot* 2013;66:361–364.
3. **Heeb S, Fletcher MP, Chhabra SR, Diggle SP, Williams P et al.** Quinolones: from antibiotics to autoinducers. *FEMS Microbiol Rev* 2011;35:247–274.
4. **Wang Y, Wilks JC, Danhorn T, Ramos I, Croal L et al.** Phenazine-1-carboxylic acid promotes bacterial biofilm development via ferrous iron acquisition. *J Bacteriol* 2011;193:3606–3617.
5. **Price-Whelan A, Dietrich LE, Newman DK.** Pyocyanin alters redox homeostasis and carbon flux through central metabolic pathways in *Pseudomonas aeruginosa* PA14. *J Bacteriol* 2007;189:6372–6381.
6. **Dietrich LE, Teal TK, Price-Whelan A, Newman DK.** Redox-active antibiotics control gene expression and community behavior in divergent bacteria. *Science* 2008;321:1203–1206.
7. **Sheplock R, Recinos DA, Mackow N, Dietrich LE, Chander M.** Species-specific residues calibrate SoxR sensitivity to redox-active molecules. *Mol Microbiol* 2013;87:368–381.
8. **Singh AK, Shin JH, Lee KL, Imlay JA, Roe JH.** Comparative study of SoxR activation by redox-active compounds. *Mol Microbiol* 2013; 90:983–996.
9. **Naseer N, Shapiro JA, Chander M.** RNA-Seq analysis reveals a six-gene SoxR regulon in Streptomyces coelicolor. *PLoS One* 2014;9:e106181.
10. **Hidalgo E, Demple B.** Spacing of promoter elements regulates the basal expression of the soxS gene and converts SoxR from a transcriptional activator into a repressor. *Embo J* 1997;16:1056–1065.
11. **Watanabe S, Kita A, Kobayashi K, Miki K.** Crystal structure of the [2Fe-2S] oxidative-stress sensor SoxR bound to DNA. *Proc Natl Acad Sci USA* 2008;105:4121–4126.
12. **Gu M, Imlay JA.** The SoxRS response of *Escherichia coli* is directly activated by redox-cycling drugs rather than by superoxide. *Mol Microbiol* 2011;79:1136–1150.
13. **Sakhtah H, Koyama L, Zhang Y, Morales DK, Fields BL et al.** The *Pseudomonas aeruginosa* efflux pump MexGHI-OpmD transports a natural phenazine that controls gene expression and biofilm development. *Proc Natl Acad Sci USA* 2016;113:E3538–E3547.
14. **Dietrich LE, Price-Whelan A, Petersen A, Whiteley M, Newman DK.** The phenazine pyocyanin is a terminal signalling factor in the quorum sensing network of *Pseudomonas aeruginosa*. *Mol Microbiol* 2006;61:1308–1321.
15. **Hernandez ME, Kappler A, Newman DK.** Phenazines and other redox-active antibiotics promote microbial mineral reduction. *Appl Environ Microbiol* 2004;70:921–928.
16. **Dietrich LE, Okegbe C, Price-Whelan A, Sakhtah H, Hunter RC et al.** Bacterial community morphogenesis is intimately linked to the intracellular redox state. *J Bacteriol* 2013;195:1371–1380.
17. **Kempes CP, Okegbe C, Mears-Clarke Z, Follows MJ, Dietrich LE.** Morphological optimization for access to dual oxidants in biofilms. *Proc Natl Acad Sci USA* 2014;111:208–213.
18. **Bertani G.** Lysogeny at mid-twentieth century: P1, P2, and other experimental systems. *J Bacteriol* 2004;186:595–600.
19. **Shanks RM, Caiazza NC, Hinsa SM, Toutain CM, O'Toole GA.** *Saccharomyces cerevisiae*-based molecular tool kit for manipulation of genes from gram-negative bacteria. *Appl Environ Microbiol* 2006;72:5027–5036.
20. **Recinos DA, Sekedat MD, Hernandez A, Cohen TS, Sakhtah H et al.** Redundant phenazine operons in *Pseudomonas aeruginosa* exhibit environment-dependent expression and differential roles in pathogenicity. *Proc Natl Acad Sci USA* 2012;109:19420–19425.
21. **Hoang TT, Karkhoff-Schweizer RR, Kutchma AJ, Schweizer HP.** A broad-host-range Flp-FRT recombination system for site-specific excision of chromosomally-located DNA sequences: application for isolation of unmarked *Pseudomonas aeruginosa* mutants. *Gene* 1998;212:77–86.
22. **Kelley LA, Mezulis S, Yates CM, Wass MN, Sternberg MJ.** The Phyre2 web portal for protein modeling, prediction and analysis. *Nat Protoc* 2015;10:845–858.
23. **Sciara G, Kendrew SG, Miele AE, Marsh NG, Federici L et al.** The structure of ActVA-Orf6, a novel type of monooxygenase involved in actinorhodin biosynthesis. *Embo J* 2003;22:205–215.

24. **Schrödinger, LLC.** The PyMOL Molecular Graphics System, Version 2.0.

25. **Parsons JF, Greenhagen BT, Shi K, Calabrese K, Robinson H** *et al.* Structural and functional analysis of the pyocyanin biosynthetic protein PhzM from *Pseudomonas aeruginosa*. *Biochemistry* 2007;46:1821–1828.

26. **Winsor GL, Griffiths EJ, Lo R, Dhillon BK, Shay JA** *et al.* Enhanced annotations and features for comparing thousands of *Pseudomonas* genomes in the *Pseudomonas* genome database. *Nucleic Acids Res* 2016;44:D646–D653.

27. **Mavrodi DV, Peever TL, Mavrodi OV, Parejko JA, Raaijmakers JM** *et al.* Diversity and evolution of the phenazine biosynthesis pathway. *Appl Environ Microbiol* 2010;76:866–879.

28. **Sakhtah H, Price-Whelan A, Dietrich L.** Regulation of phenazine biosynthesis. In: *Microbial Phenazines*. Berlin, Heidelberg: Springer; 2013. pp. 19–42.

29. **Madsen JS, Lin YC, Squyres GR, Price-Whelan A, de Santiago Torio A** *et al.* Facultative control of matrix production optimizes competitive fitness in *Pseudomonas aeruginosa* PA14 biofilm models. *Appl Environ Microbiol* 2015;81:8414–8426.

30. **Kendrew SG, Hopwood DA, Marsh EN.** Identification of a monooxygenase from *Streptomyces coelicolor* A3(2) involved in biosynthesis of actinorhodin: purification and characterization of the recombinant enzyme. *J Bacteriol* 1997;179:4305–4310.

31. **Yang JY, Phelan VV, Simkovsky R, Watrous JD, Trial RM** *et al.* Primer on agar-based microbial imaging mass spectrometry. *J Bacteriol* 2012;194:6023–6028.

32. **Turner JM, Messenger AJ.** Occurrence, biochemistry and physiology of phenazine pigment production. *Adv Microb Physiol* 1986;27:211–275.

33. **Mavrodi DV, Bonsall RF, Delaney SM, Soule MJ, Phillips G** *et al.* Functional analysis of genes for biosynthesis of pyocyanin and phenazine-1-carboxamide from *Pseudomonas aeruginosa* PAO1. *J Bacteriol* 2001;183:6454–6465.

34. **Wang Y, Newman DK.** Redox reactions of phenazine antibiotics with ferric (hydr)oxides and molecular oxygen. *Environ Sci Technol* 2008;42:2380–2386.

35. **Bellin DL, Sakhtah H, Rosenstein JK, Levine PM, Thimot J** *et al.* Integrated circuit-based electrochemical sensor for spatially resolved detection of redox-active metabolites in biofilms. *Nat Commun* 2014;5:3256.

36. **Zheng H, Kim J, Liew M, Yan JK, Herrera O** *et al.* Redox metabolites signal polymicrobial biofilm development via the NapA oxidative stress cascade in *Aspergillus*. *Curr Biol* 2015;25:29–37.

37. **Okegbe C, Price-Whelan A, Dietrich LE.** Redox-driven regulation of microbial community morphogenesis. *Curr Opin Microbiol* 2014; 18:39–45.

38. **Okegbe C, Fields BL, Cole SJ, Beierschmitt C, Morgan CJ** *et al.* Electron-shuttling antibiotics structure bacterial communities by modulating cellular levels of c-di-GMP. *Proc Natl Acad Sci USA* 2017;114:E5236–E5245.

39. **Lin YC, Sekedat MD, Cornell WC, Silva GM, Okegbe C** *et al.* Phenazines regulate Nap-dependent denitrification in *Pseudomonas aeruginosa* biofilms. *J Bacteriol* 2018.

Edited by: S. P. Diggle and M. Whiteley